FABRICATION OF AN ALUMINUM BASED HOT ELECTRON MIXER FOR TERAHERTZ APPLICATIONS

P. M. Echternach, H.G. LeDuc, A. Skalare and W.R. McGrath
Center for Space Microelectronics Technology, Jet Propulsion Laboratory,
California Institute of Technology, Pasadena, CA, 91109-8099

ABSTRACT

Aluminum based diffusion cooled hot electron bolometers (HEB) mixers, predicted to have a broader bandwidth, to require less LO power, and perhaps even have lower noise than Nb based diffusion cooled HEBs, have been fabricated. Preliminary DC tests were performed. The bolometer elements consisted of short (0.18 to 0.53 μm), narrow (0.08 to 0.15 μm) and thin (11 nm) aluminum microbridges connected to large contact pads consisting of a novel trilayer Al/Ti/Au. The patterns were defined by electron beam lithography and the metal deposition involved a double angle process, with the aluminum microbridges being deposited at –degree (i.e. straight on) and the pads being deposited at a 45 degree angle without breaking vacuum. The Al/Ti/Au trilayer was developed to provide a way of making contact between the aluminum microbridge and the gold antenna without degrading the properties of the microbridge. The titanium layer acts as a diffusion barrier to avoid damage of the aluminum contact and bolometer microbridge and to lower the transition temperature of the pads to below that of the bolometer microbridge. The Au layer avoids the formation of an oxide on the Ti layer and provides good electrical contact to mixer rf embedding circuit and planar antenna. The resistance of the bolometers as a function of temperature was measured. It appears that below the transition temperature of the microbridge (1.8K) but above the transition temperature of the contact pads (0.6K), the proximity effect drives much of the bolometer microbridge normal, which gives the apperance of a very broad transition. This however should not affect the performance of the bolometers since they will be operated at a temperature below the Tc of the pads, and hence no proximity effect will be present. This is evident from the IV characteristics measured at 0.3K. RF characterization tests will begin shortly.

INTRODUCTION

Hot electron bolometric mixers , both phonon[1,2] or diffusion[3,4] cooled have become a very attractive choice for heterodyne detection above 1 THz, in terms of temperature noise and LO power. However, requirements and constraints of future missions and applications will benefit from even lower LO power, higher bandwidth, and lower noise temperatures. It has been predicted that aluminum-based diffusion cooled bolometers might have better performance in all counts. Absorbed LO power, which is proportional to the square of the transition temperature and inversely proportional to the device resistance, could be a factor of at least5 to 10 times lower than either Nb or NbN for optimized devices.[5] In terms of IF bandwidth, aluminum should also be better due to its higher diffusion constant, having the potential to yield bandwidths of several tens of GHz.

We have now fabricated and performed DC characterization on Al-based hot electron bolometers. The DC characterization reveals that the devices are well within the design parameter space for optimal performance.[5] RF characterization will start shortly.

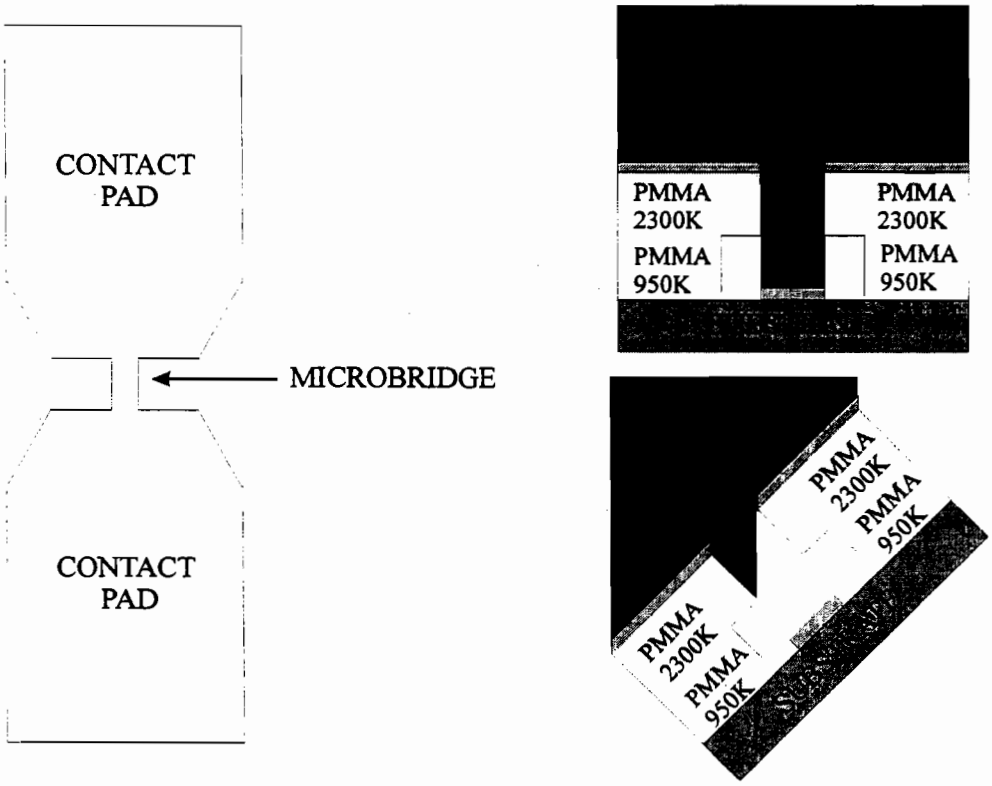

Figure 1. *Schematic drawing of microbridge and its cross section. The microbridge materal is deposited straight on and the pads at a 45 degree angle.*

FABRICATION PROCESS

The devices were fabricated on 3 inch silicon wafers with a 20 nm thermally grown silicon oxide layer. The microbridge and contact pad patterns were defined by electron beam lithography on a double layer PMMA structure. Since the bottom layer (140 nm thick 950K PMMA) is more sensitive than the top (120nm 2300K PMMA) an undercut profile is achieved upon developing in a MIBK:IPA 1:3 solution for 90 seconds. The microbridge width varied from 80nm to 140 nm. Metal depositions are performed in an electron beam evaporator with a base pressure of $3x10^{-6}$ Pa equipped with a tilt stage that allows evaporations at two angles. The microbridge material (11 nm Al) is evaporated with the substrate perpendicular to the material flux. The contact pad material (63nm Al/28nm Ti/28nm Au) is evaporated at a 45 degree angle. This ensures that the contact pad material hits the PMMA vertical wall in the microbridge region as depicted in Figure 1. Lift off in acetone is performed next. Note that this process results in a 0.25μm inconsequential misalignment between the contact pads and the microbridge.
The twin slot antennas and RF filter circuits are defined next using a process developed for Nb HEB devices[6]. The layer composition is 500nm Polyimide/40nm Nb/130 nm PMMA9500K/ 120nm PMMA 2300K. Electron beam lithography followed by chromium

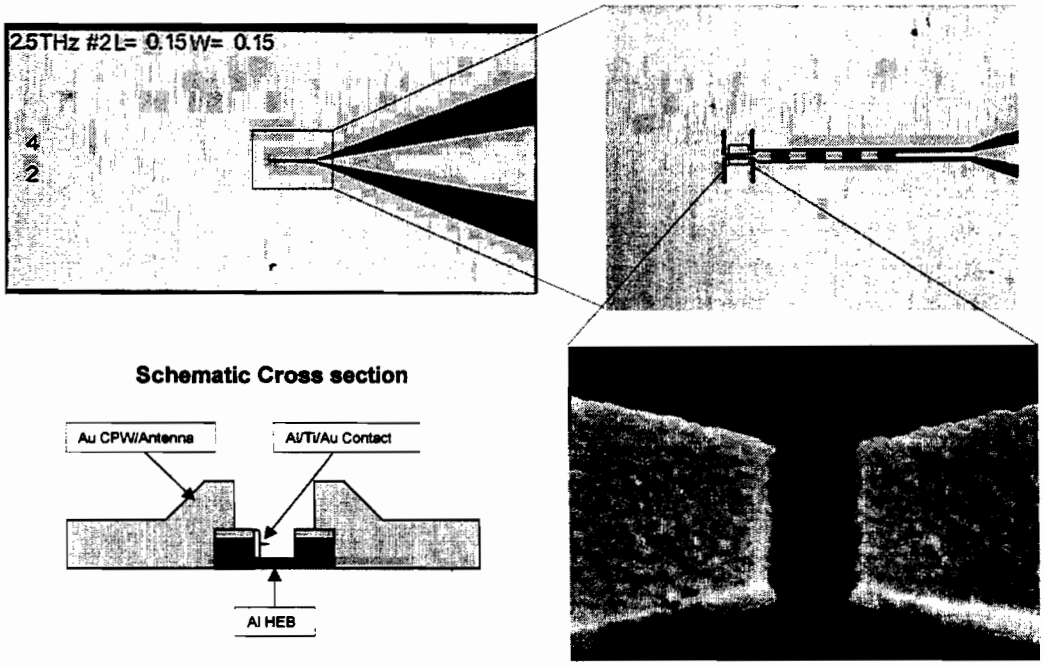

Figure 2. *Pictures of finished Al based hot electron bolometer and schematic representation of layer structure.*

deposition and lift off in acetone is used to define an etch mask for the high resolution portion of the twin slot antennas and RF filter circuit. A matching photoresist mask for the low resolution portion is defined by standard photolithography using AZ5214 photo-resist. With chromium and photoresist as a composite mask, the Nb in exposed areas is etched with CF4 +10%O_2 and the polyimide with pure 0_2. This is followed by deposition of 2.5 nm Ti and 300 nm Au. The last step is lift-off in methylene Chloride. Figure 2 shows a finished device and its layer composition.

ELECTRICAL CHARACTERIZATION

Resistance versus temperature and I-V characteristics of a number of devices were measured. The table shows a summary of resistance measurements at room temperature and at 2K. The actual dimensions were measured from SEM micrographs. The difference between design and actual dimensions is due to an over-compensation for the over-sizing inherent to the electron beam lithography process and will be corrected for the next iteration. The uncertainty in each dimension measurement is 10% yielding a 20% uncertainty in the R values. The average value is roughly 51 Ω, which would provide a good match for the IF amplifier for a microbridge containing one or two squares. This should yield a diffusion constant D□10 cm^2 and is well within the desired range of the design parameters.[7]

Device	Antenna	Design dim.		Actual dim.		R_{300K} (Ω)	R_{2K} (Ω)	R_{2K} (Ω)
		L(μm)	W(μm)	L(μm)	W(μm)			
1	1.9THz	0.3	0.15	0.35	0.14	128	90	36±7
2	1.9Thz	0.2	0.1	0.25	0.08	149	108	35±7
3	1.9THz	0.15	0.15	0.25	0.14	159	120	67±14
4	4.25THz	0.2	0.1	0.27	0.08	175	133	40±8
5	1.9THz	0.2	0.1	0.27	0.08	251	190	56±11
6	2.5THz	0.1	0.1	0.18	0.08	204	162	72±14
7	1.9THz	0.3	0.15	0.35	0.14	195	135	54±10

The resistance of the devices was measured as a function of temperature down to 0.3K. Figure 3 shows the results for three devices with different lengths. The curves were normalized to the resistance at 2K of the shortest sample. The curves feature a broad transition starting at 1.8K(which would be roughly the transition temperature of the microbridge film) and a second sharper transition at 0.6K, which is the transition temperature of the contact pads. Since the second transition features a large drop in resistance, it can not be due to the resistance of the contact pads. It must be that a large portion of the link undergoes a superconducting transition at that temperature. The contact pads while in the normal state are driving a significant portion of the microbridge normal through the proximity effect. As the temperature is lowered, gradually larger

portions of the microbridge become superconducting, lowering the overall resistance. This explains the broad transition. Note that the shortest sample features the largest fractional drop in resistance at 0.6K and the longest shows the smallest effect. This is consistent with our explanation and provides a rough measurement of the normal metal coherence length ξ_N. For the sake of simplicity, we assume that the center of the microbridge is superconducting at 0.6K, and divide it in two halves. The coherence length would be roughly equal to the normal length of a half bridge, if we assume that the proximity effect acts up to a distance roughly equal to the coherence length. For the 180 nm bridge this would be roughly 90 nm, since the resistance drop at 0.6K is about equal to the total normal resistance, i.e. ξ_N =90nm. For the 270 nm it would be $\xi_N \approx \frac{55\Omega}{90\Omega}\frac{270nm}{2} = 83nm$. For the 350 nm bridge it would be $\xi_N \approx \frac{40\Omega}{90\Omega}\frac{350nm}{2} = 78nm$. Using the average value, we would have ξ_N= 84 nm,

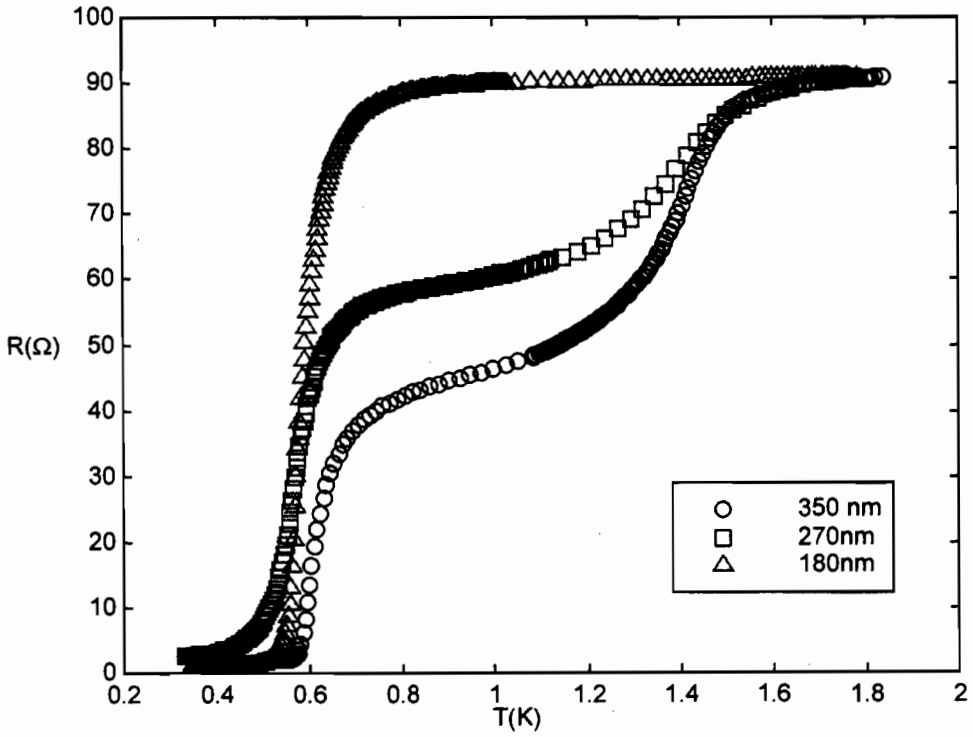

Figure 3. *Resistance vs temperature of selected devices. All values were normalized to the values of the shortest microbridge at 2K.*

yielding a diffusion constant $D = \frac{k_B T}{\hbar} \xi_N^2 \cong 6\text{cm}^2/\text{s}$, which is consistent with the value of D estimated from the resistance. Attempts to model the data using results for the proximity effect in bulk materials provide qualitative but not quantitative agreement, which is not surprising since all the dimensions in this case are smaller than or comparable to the normal metal coherence length. We have tried to fit our data using the charge imbalance and Andreev reflection model developed for Nb devices[8], which could be viewed as a microscopic picture of the proximity effect. Again, the agreement was qualitative, at best.

Even though the resistance vs temperature characteristics of the bolometers has such broad features that at first glance would be undesirable, in actual operation the mixers would be kept below the transition temperature of the pads. At those temperatures the pads are superconducting and the signal would "see" just the superconducting microbridge. This is corroborated by IV characteristics measured at 0.3K. One such IV characteristic is shown in figure 4.

To check that the transition temperature of the pads was at 0.6K we fabricated macroscopic samples with the same layer composition and measured its transition temperature obtaining a value of 0.67 K. The agreement is reasonable, since in additional

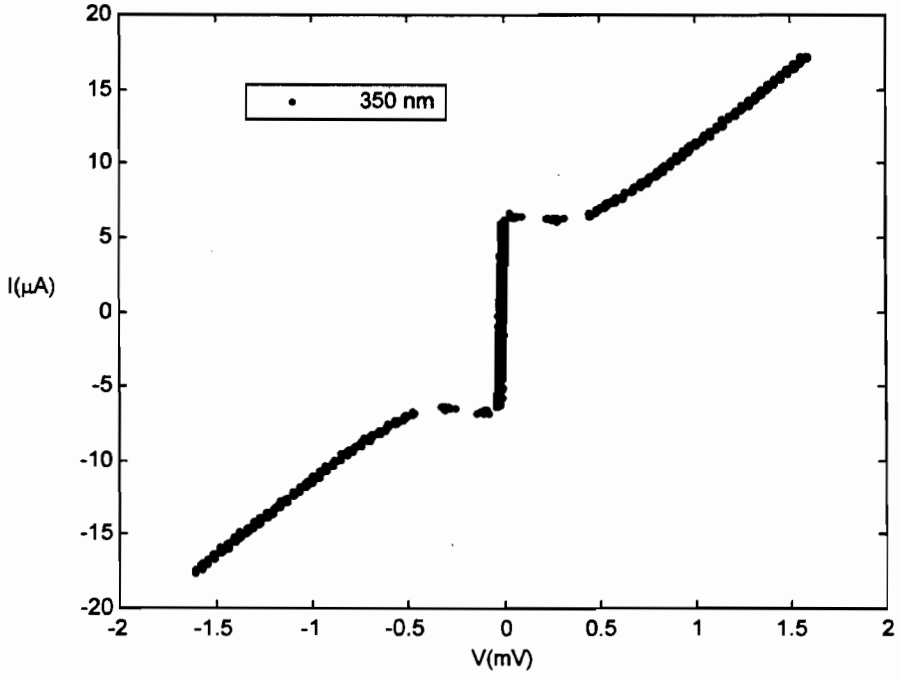

Figure 4. *I-V characteristic of 350nm long Al based HEB*

to the precision of the layer thickness measurement (10%) there is an additional uncertainty due to the evaporation at an angle. Not only the angle has an uncertainty but also the thickness should vary across the wafer, since the distance to the evaporation source varies. We fabricated and measured the transition temperatures of samples with thicknesses of Al ranging from 100 to 630 Å for fixed thicknesses of Ti (280Å) and Au (280Å). Figure 5 shows the results, indicating that we can tailor the Tc of this trilayer from 350 mK up making it very useful for applications such as transition edge sensors. We have also fabricated one sample without an Au layer to demonstrate that the Au layer has an influence on the Tc and is not just acting as a normal metal layer on top of the Al/Ti proximity layer. This confirmation is important for applications in which this normal layer would be undesirable. We have also heated some of the samples up to 170C for 10 minutes and measured their characteristics afterwards with no discernible changes. This makes the Al/TiAg superior to Al/Ag bilayers, which are extremely sensitive to heating, making them unsuitable for applications in which processing is necessary after the deposition of the film.

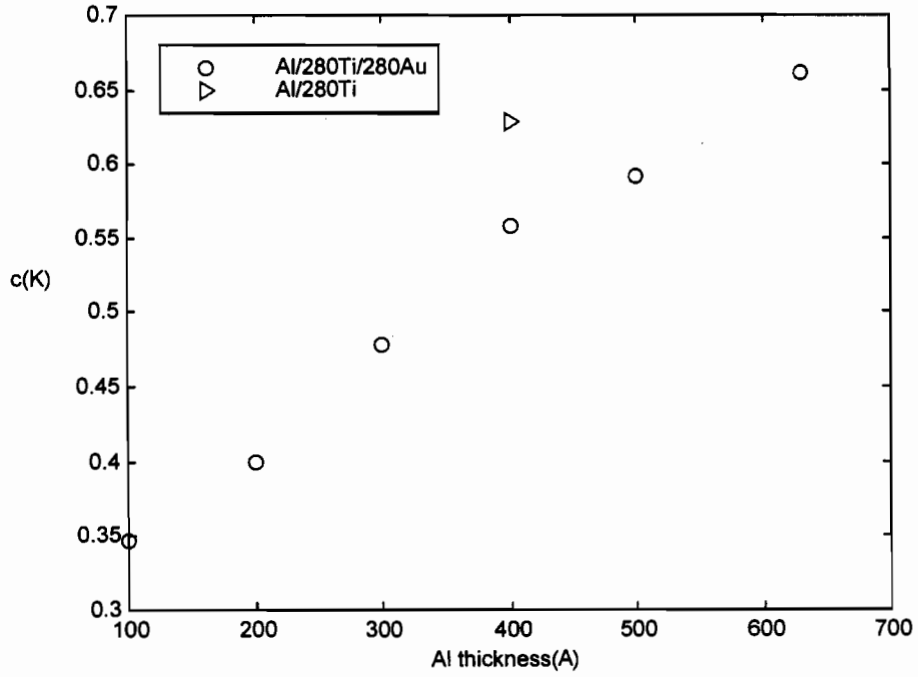

Figure 5. *Transition temperatures of Al/Ti/Au trilayers as a function of Al thickness.*

CONCLUSION

We have fabricated aluminum based hot electron bolometers to be used as mixers at 1.9 and 2.5THz. DC electrical characterization shows that the devices are within the design parameters. A novel trilayer Al/Ti/Au was developed to provide contact between the microbridge and the antenna structures. This trilayer is superior to Al/Ag bilayers due to its insensitivity to heating.

This research is supported by the Center for Space Microelectronic Technology, Jet Propulsion Laboratory under contract to the National Aeronautics and Space Administration, Office of Space Science.

---

[1] E. Gerecht, C.F. Musante, H. Jian, K.S. Yngvesson, J. Dickinson, J. Waldman, G.N. Gol'tsman, P.A. Yagoubov, B.M. Voronov, E.M. Gershenzon, , Proceedings of the Ninth International Symposium on Space Terahertz Technology, pp 105-114 (1998) and references therein.

[2] Y.P. Gousev, H.K. Olson, G.N. Gol'tsman, B.M. Voronov, E.M. Gershenzon, Proceedings of the Ninth International Symposium on Space Terahertz Technology, pp 121-130 (1998), and references therein.

[3] P.J. Burke, R.J. Schoelkopf, I. Siddiqi, D.E. Prober, A. Skalare, B.S. Karasik, M.C. Gaidis, W.R. McGrath, B.Bumble, H.G. LeDuc, Proceedings of the Ninth International Symposium on Space Terahertz Technology, pp 17-34 (1998), and references therein.

[4] A.Skalare, W.R. McGrath, B. Bumble, H.G. LeDuc, Proceedings of the Ninth International Symposium on Space Terahertz Technology, pp 115-120 (1998), and references therein.

[5] B.S. Karasik and W.R. McGrath, Proceedings of the Ninth International Symposium on Space Terahertz Technology, pp 73-80 (1998).

[6] B.Bumble and H.G. LeDuc, IEEE Transaction on Applied Superconductivity 7, 105 (1997)

[7] Estimate of D from figure 4 in reference 5.

[8] D.W. Floet , J.J. Baselmans, J.R. Gao T.M. Klapwijk, Proceedings of the Ninth International Symposium on Space Terahertz Technology, pp 63-72 (1998).